A Dynamic Model of Photoproduction, Photoregulation and Photoinhibition in Microalgae using Chlorophyll Fluorescence

Andreas Nikolaou * Andrea Bernardi ** Fabrizio Bezzo **
Tomas Morosinotto *** Benoît Chachuat *

* Centre for Process Systems Engineering, Department of Chemical
Engineering, Imperial College London, South Kensington Campus,
London, SW7 2AZ, UK
e-mail: {andreas.nikolaou10,b.chachuat}@imperial.ac.uk
** CAPE-Lab – Computer-Aided Process Engineering Laboratory,
Department of Industrial Engineering, University of Padova,
via Marzolo 9, 35131 Padova, Italy
e-mail: andrea.bernardi.7@studenti.unipd.it,
fabrizio.bezzo@unipd.it
*** Department of Biology, University of Padova, 35131 Padova, Italy
e-mail: tomas.morosinotto@unipd.it

Abstract: Fluorescence is a powerful tool for observing and understanding photosynthetic processes in microalgae. This paper presents a dynamic model describing key photosynthetic processes, whose predictions can be related to the characteristic fluorescence fluxes arising from Pulsed Amplitude Modulation (PAM) protocols. The mechanistic model by Han is used as a building block for predicting photoproduction and photoinhibition, and an extension is proposed in order to encompass a particular type of photoregulation, namely qE quenching. Moreover, the lake model—a specific type of Photosystem II arrangement—is considered in formulating the quantum yield of fluorescence, which leads to simple expressions of the characteristic fluorescence fluxes in terms of the model variables. A first calibration and validation of the model is performed against experimental data, showing excellent agreement.

Keywords: modeling; fluorescence; microalgae; non-photochemical quenching; photoinhibition

1. INTRODUCTION

Microalgae have long been identified a promising candidate for biofuel production (Sheehan et al., 1998). These microorganisms have fast growth rates and a rich protein content, in addition to being able to produce and accumulate lipids under certain stress conditions (Mutanda et al., 2011). They are considered by many a viable alternative to conventional oil crops due to a higher biomass productivity and independence towards arable land and fresh water (Chisti, 2007). Moreover, the downstream processing of microalgae in biorefineries opens the perspective for producing a wide spectrum of valuable products in addition to biofuel, including cosmetics, pharmaceuticals and nutraceuticals (Metting, 1996), while treating nutrient-rich effluents from wastewater treatment works (Pittman et al., 2011) or CO_2 from power plant flue gas (Benemann, 1997), all in the same process. Despite these promises, mass production of microlagae for large-scale biofuel production is yet to be demonstrated, especially in regards of their

high nutrient requirements, the trade-off between biomass growth and lipid productivity, and the lipid extraction challenges (le B. Williams and Laurens, 2010).

In this context, the development of mathematical models that are capable of predicting the behavior of a microalgae culture accurately is paramount. At a fundamental level, models used in conjunction with experiments are invaluable tools to unveil and untangle the underlying photosynthetic and metabolic mechanisms. For process development purposes likewise, models can be used to improve the design, operation and control of a microalgae culture in order to enable and sustain a higher biomass production or lipid content. The processes governing microalgae growth are intricate and span multiple time scales, ranging from milliseconds to days: *Photoproduction* encompasses all the processes from photons utilization to CO_2 fixation that occur within milliseconds (le B. Williams and Laurens, 2010); *Photoinhibition*, the observed loss of photosynthetic production due to excess or prolonged exposure to light, acts on a time scale of minutes to hours (Han, 2002); *Photoregulation*, also referred to as *Non Photochemical Quenching* (NPQ), the set of mechanisms by which microalgae protect their photosynthetically-active components via the dissipation of excess energy as heat, occurs within minutes (Müller et al., 2001); *Photoacclimation*, the

ability of the cells to adjust their pigment content and composition under varying light and nutrient conditions, occurs within hours or days (MacIntyre et al., 2002). Finally, the mechanisms involved in nutrient internalization and their metabolism into useful products occurs within hours or days as well (Falkowski and Raven, 1997).

Chlorophyll-a fluorescence is a powerful tool for the analysis of the aforementioned processes, which has led to important discoveries over the past 40 years. Today's state-of-the-art equipments, such as Pulse Amplitude Modulation (PAM), can implement complex protocols with great measurement accuracy. In order to fully exploit this capability, experimental protocols have been developed that relate the measured fluorescence fluxes with key photosynthetic parameters such as the quantum yield of photosynthesis, the photosynthetic apparatus activity, and the NPQ activity. But even though the level of understanding of the various fluorescence measures has improved significantly over the past few years, little effort has been devoted to developing dynamic models that relate specific photosynthetic mechanisms to those parameters.

The main objective of this paper is to develop a mathematical model that can predict the fluorescence fluxes in terms of the photosynthetic mechanisms occurring inside the chloroplasts. This model builds upon the widely-accepted state-transition model proposed by Han (2002) for predicting photoproduction and photoinhibition. An extension of this model in the form of a semi-empirical expression is proposed in order to encompass a particular type of photoregulation, namely *qE quenching*. Moreover, the chlorophyll-a fluorescence flux is expressed based on the work by Huot and Babin (2010), for a specific type of Photosystem II arrangement, the so-called *lake model*. The novelty and originality of the model lies in the way the states of the PSUs, as given by the (extended) Han model, are related to the measured fluorescence parameters, and how it does so by accounting for qE quenching.

The remainder of the paper is organized as follows. The principles of fluorescence are briefly discussed in Sect. 2. The dynamic model is then presented in Sect. 3, including a description of the Han model and an extension of this model to encompass photoregulation, a description of the fluorescence flux and fluorescence yield, and a derivation of key model properties. A preliminary validation of the model and discussion of the results follows in Sect. 4. Finally, Sect. 5 concludes the paper and discusses future research directions.

2. PRINCIPLES OF CHLOROPHYLL FLUORESCENCE

2.1 Fluorescence Measurement Protocols

Chlorophyll fluorescence refers to the re-emission of photons previously absorbed by chlorophyll molecules at a fixed wavelength of 668 nm (Huot and Babin, 2010). This property, combined with energy balance considerations, is very handy in studying photosynthesis. More precisely, the photons absorbed by chlorophyll molecules undergo either one of three fates; they are either used in photosynthetic reactions (photoproduction), dissipated as heat (photoregulation), or re-emitted (fluorescence). Accord-

ingly, much information about photosynthetic processes can be inferred via measurement of the fluorescence flux under specific lighting protocols that preferably activate or inactivate either photoproduction or photoregulation.

Among the available fluorescence techniques, the focus here is on Pulsed Amplitude Modulation (PAM). A PAM protocol consists of a sequence of light events that trigger various photosynthetic processes in a given solution sample containing microalgae. A distinct light source, called *actinic light*, is used to excite—that is, reduce—the photosynthetic apparatus and another source, called *measuring light*, is used to measure fluorescence. The measuring light is weak enough that it does not cause any significant reduction of the photosynthetic apparatus. The outcome of a PAM protocol is a record of fluorescence flux against time, which provides the following characteristic fluxes:

- *Dark-adapted, minimum fluorescence flux, F_0*: The measuring light is applied to a sample that has been kept in the dark. The photosynthetic apparatus is completely oxidized (zero excitation state) and the NPQ processes are inactive.
- *Dark-adapted, maximum fluorescence flux, F_m*: The measuring light is applied, after a short and intense actinic light pulse, to a sample that has been kept in the dark. The photosynthetic apparatus is completely reduced (maximal excitation state), while the NPQ processes remain inactive.
- *Light-adapted, minimum fluorescence flux, F_0'*: The measuring light is applied to a sample that has been exposed to a constant actinic light, after switching off the actinic light. The photosynthetic apparatus is completely oxidized and the NPQ processes are now active.
- *Light-adapted, maximum fluorescence flux, F_m'*: The measuring light is applied, after a short and intense actinic light pulse, to a sample that has been exposed to a constant actinic light. The photosynthetic apparatus is completely reduced and the NPQ processes are active.
- *Light-adapted, steady-state fluorescence flux, F'*: The measuring light is applied to a sample that has been exposed to a constant actinic light. The photosynthetic apparatus is only partially reduced (realized excitation state) and the NPQ processes are active.

2.2 Fluorescence Indexes

The main fluorescence *indexes*, often referred to as fluorescence *parameters* in the literature, are expressed as combinations of the characteristic fluxes F_0, F_m, F_0', F_m' and F'. By discriminating either between dark- and light-adapted states, or between zero, realized and maximal excitation states, these indexes allow quantification of the various photosynthetic processes.

The maximum quantum yield of photosynthesis, q, considers dark-adapted states and is given by (Baker, 2008):

$$q = \frac{F_m - F_0}{F_m}. \tag{1}$$

In contrast, the realized quantum yield of photosynthesis, $\Phi_{PS2}(I,t)$, at given actinic light intensity I and time instant t, considers light-adapted states and is given by:

$$\Phi_{\mathrm{PS2}}(I,t) = \frac{F'_{\mathrm{m}}(I,t) - F'(I,t)}{F'_{\mathrm{m}}(I,t)} \, . \qquad (2)$$

This index is also known as the *Genty parameter*, after the researcher who first derived it (Genty et al., 1989).

Another fluorescence index, $q_{\mathrm{P}}(I,t)$, considers the level of excitation of the photosynthetic apparatus as a means to quantify the extent of photochemical quenching (Maxwell and Johnson, 2000):

$$q_{\mathrm{P}}(I,t) = \frac{F'_{\mathrm{m}}(I,t) - F'(I,t)}{F'_{\mathrm{m}}(I,t) - F'_0(I,t)} \, . \qquad (3)$$

A related index, $q_{\mathrm{L}}(I,t)$, is considered by Kramer et al. (2004) for describing interconnections within the photosynthetic apparatus:

$$q_{\mathrm{L}}(I,t) = q_{\mathrm{P}}(I,t) \frac{F'_0(I,t)}{F'(I,t)} \, . \qquad (4)$$

Fluorescence indexes describing the extent of photoregulation can be derived likewise. The difference between $F'_{\mathrm{m}}(I,t)$ and F_{m} represents the dissipation of energy due to photoregulation. Bilger and Björkman (1990) formulate the NPQ index via scaling of this difference term by $F'_{\mathrm{m}}(I,t)$. In the following, we consider the equivalent index

$$q_{\mathrm{NPQ}}(I,t) = \frac{F_{\mathrm{m}} - F'_{\mathrm{m}}(I,t)}{F_{\mathrm{m}}} \, , \qquad (5)$$

where scaling is with respect to F_{m} instead of $F'_{\mathrm{m}}(I,t)$, in order for the resulting index to lie between 0 and 1.

3. DYNAMIC MODEL OF FLUORESCENCE

3.1 Han Model

The model developed by Han (2002) is based on the concept of Photosynthetic Units (PSU). A PSU is comprised of an *antenna* complex made up of pigments that is associated with the *reaction center* of a Photosystem II (RCII). The antenna absorbs the incoming photons and triggers electronic excitation, eventually leading to oxygen production in the RCII. In this conceptual representation, the chloroplasts in microalgae are seen as PSU arrays.

The description of photoproduction and photoinhibition in the Han model assumes that the RCII can be in either one of three states, namely open (A), closed (B) and damaged (C). An RCII in state A is completely oxidized; in state B, completely reduced; and in state C, nonfunctional. Depending on the light intensity, each RCII can transit from one state to another, with processes described by first-order kinetics, as depicted in Fig. 1.
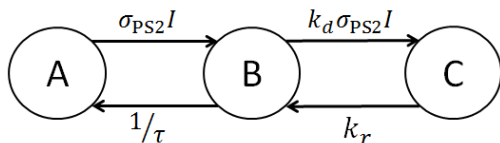

Fig. 1. Schematic representation of the Han model

Photoproduction is described by the transition from A to B, while the reverse transition from B to A represents the relaxation of RCII. Photoinhibition, on the other hand, corresponds to the transition from B to C, while the

reverse transition from C to B describes the repair of damaged RCII by enzymatic processes.

The equations describing the dynamics of open, closed and damaged states are expressed in terms of the probabilities $A(t)$, $B(t)$ and $C(t)$ that sum up to 1 at every time:

$$\dot{A} = -I\,\sigma_{\mathrm{PS2}}\,A + \frac{B}{\tau}$$

$$\dot{B} = I\,\sigma_{\mathrm{PS2}}\,A - \frac{B}{\tau} + k_{\mathrm{r}}\,C - k_{\mathrm{d}}\,\sigma_{\mathrm{PS2}}\,I\,B \qquad (6)$$

$$\dot{C} = -k_{\mathrm{r}}\,C + k_{\mathrm{d}}\,\sigma_{\mathrm{PS2}}\,I\,B \, .$$

Here, σ_{PS2} denotes the effective cross section $[\mathrm{m}^2\,\mu\mathrm{E}^{-1}]$; τ, the turnover time $[\mathrm{s}]$; k_{d}, the damage rate constant [dimensionless]; and k_{r}, the repair rate constant $[\mathrm{s}^{-1}]$.

3.2 Accounting for Photoregulation in the Han Model

On time scales where the processes of photoregulation and photoacclimation are negligible and where the nutrient status remains about constant, the parameters σ_{PS2}, τ, k_{d} and k_{r} in the Han model (6) can themselves be considered constant. Nonetheless, the assumption of a negligible photoregulation contribution may not hold in the time scale of a PAM protocol, which typically runs over several minutes. The ability to predict such protocols thus hinges on an extension of the Han model.

The focus in this paper is on the prominent type of NPQ regulation, namely energy-dependent quenching— qE quenching in short. This particular regulation refers to the reversible interconversion of xanthophylls (oxygenated carotenoids), triggered by the strong proton (H^+) gradient that develops across the thylakoid membrane under saturating light irradiance (Bilger and Björkman, 1990). This interconversion, known as the xanthophyll cycle, acts on time scales ranging from seconds up to several minutes, and it can cause up to 90% reduction in the fluorescence flux (Huot and Babin, 2010).

The effect of qE quenching comes forward through the variation in photon absorption by the antenna. A natural way of modeling this effect is therefore in terms of the total cross section, σ, the photosynthetic parameter capturing the light absorption effectiveness most directly. More specifically, we assume that σ is bounded between a maximum value, $\sigma_{\max}$, and a minimal value, $\sigma_{\min}$, which are observed when the NPQ energy dissipation is, respectively, the lowest and the highest:

$$\sigma = \sigma_{\max}\,(1-\alpha) + \sigma_{\min}\,\alpha \, . \qquad (7)$$

Here, α represents the NPQ activity at a given time instant, bounded between 0 and 1. As a first approximation, we assume that α follows first-order dynamics,

$$\dot{\alpha} = \xi\,(\alpha_{\mathrm{ss}}(I) - \alpha) \, , \qquad (8)$$

with ξ standing for the characteristic time of the qE quenching dynamics; and $\alpha_{\mathrm{ss}}(I)$, the qE quenching activity, in steady state, at the actinic light level I. Experimental observations indicate that α_{ss} exhibits a switch-like behavior, which can be captured for instance by a sigmoid (Hill-type) function of the form

$$\alpha_{\mathrm{ss}}(I) := \frac{I^n}{I_{\mathrm{qE}}^n + I^n} \, , \qquad (9)$$

where I_{qE} represents the irradiance level around which the transition from minimal to maximal activity occurs, and n describes the sharpness of the switch-like transition.

In turn, the total cross section σ can be related to the corresponding parameter σ_{PS2} in the Han model (6). According to Falkowski and Raven (1997), the latter can be expressed as

$$\sigma_{PS2} = \Phi_p^A \sigma_{PSU} , \qquad (10)$$

where Φ_p^A denotes the quantum yield of photosynthesis of an open RCII, for which an expression in terms of fluorescence quantum yields will be derived later on in Sect. 3.4; and σ_{PSU}, the optical cross section, related to σ simply as

$$\sigma = \sigma_{PSU} N , \qquad (11)$$

with N the number of PSUs [$\mu E\,g_{chl}^{-1}$], assumed constant in the time scale of interest.

Combining (7), (10) and (11) yields the following expression of σ_{PS2} in terms of the photoregulation parameters:

$$\sigma_{PS2} = \frac{\Phi_p^A}{N} \left(\sigma_{max}\,(1-\alpha) + \sigma_{min}\,\alpha \right) , \qquad (12)$$

which can be used in the Han model (6) equations.

3.3 Fluorescence Quantum Yield

The fluorescence flux F, as measured by a PAM fluorometer, can be expressed as (Huot and Babin, 2010):

$$F = I_m\,\sigma\,chl\,\Phi_f\,(1-Q)\,V , \qquad (13)$$

where I_m denotes the measuring light intensity; chl, the chlorophyll concentration; Φ_f, the quantum yield of fluorescence; V, the sample volume; and Q is a parameter describing the percentage of fluorescence absorbed by the sample, which is typically assumed constant.

Several expressions of the fluorescence quantum yield Φ_f in terms of the PSU states, A, B and C, have been proposed depending on the antenna-RCII configuration. They typically involve the parameters Φ_f^A, Φ_f^B and Φ_f^C that represent the fluorescence quantum yields of a PSU in state A, B or C, respectively. Two such expressions are:

Puddle Model   This configuration assumes that each RCII has its own antenna. The fluorescence quantum yield is thus obtained as the algebraic mean of the fluorescence quantum yields of A, B and C:

$$\Phi_f := \Phi_f^A A + \Phi_f^B B + \Phi_f^C C . \qquad (14)$$

Lake Model   This configuration assumes that all RCII's are connected to a common antenna, thereby implying competition among RCII's for the incoming excitation energy. The fluorescence quantum yield is then obtained as the harmonic mean of the fluorescence quantum yields of A, B and C:

$$\Phi_f := \frac{1}{\dfrac{A}{\Phi_f^A} + \dfrac{B}{\Phi_f^B} + \dfrac{C}{\Phi_f^C}} . \qquad (15)$$

It has been reported that the Lake model can represent the actual configuration of the antenna-RCII complex more accurately (Kramer et al., 2004), and the focus shall therefore be on this model in the remainder of this paper. It has also been argued (Maxwell and Johnson, 2000) that the fraction of incoming photons leading to photoproduction in an open RCII should be the same as the fraction of incoming photons being dissipated as heat in a damaged RCII, so that $\Phi_f^A = \Phi_f^C$. This hypothesis is adopted subsequently and results in the following expression of the fluorescence quantum yield:

$$\Phi_f = \frac{1}{\dfrac{A+C}{\Phi_f^A} + \dfrac{B}{\Phi_f^B}} . \qquad (16)$$

3.4 Expressions of Fluorescence Indexes

The following properties express the various fluorescence indexes introduced in Sect. 2.2 in terms of the variables and parameters in the proposed dynamic model.

Property 1. The realized quantum yield of photosynthesis, Φ_{PS2}, is nonlinearly related to the fractions of open and closed RCII's as:

$$\Phi_{PS2}(I,t) = \frac{A\dfrac{\Phi_f^B - \Phi_f^A}{\Phi_f^B}}{1 - B\dfrac{\Phi_f^B - \Phi_f^A}{\Phi_f^B}} . \qquad (17)$$

In particular for $A = 1$, one recovers the quantum yield of photosynthesis of an open RCII, Φ_p^A, given by:

$$\Phi_p^A = \frac{\Phi_f^B - \Phi_f^A}{\Phi_f^B} . \qquad (18)$$

Property 2. The maximum quantum yield of photosynthesis, q, is linearly related to the fraction of damaged RCII at the start of the PAM protocol, C_0, as:

$$q = \Phi_p^A(1 - C_0) = \frac{\Phi_f^B - \Phi_f^A}{\Phi_f^B}(1 - C_0) . \qquad (19)$$

Property 3. The fluorescence index q_L is given by the ratio of open-to-active RCII's as:

$$q_L(I,t) = \frac{A}{A+B} . \qquad (20)$$

4. RESULTS AND DISCUSSION

A first validation of the model is conducted in this section using experimental data from a PAM fluorometer for the microalgae *Nannochloropsis Salina* (Sforza et al., 2012). These data are for a culture pre-acclimated at 46 $\mu E\,m^{-2}\,s^{-1}$ that is exposed to an actinic light intensity increasing incrementally from 0 to 1960 $\mu E\,m^{-2}\,s^{-1}$ in stages of 30 s. The total duration of the PAM experiment is 600 s, and the fluorescence fluxes $F'(I,t)$, $F_m'(I,t)$ and $F_0'(I,t)$ are recorded throughout.

For the purpose of model calibration, and due to a lack of information regarding the measuring light intensity I_m, the sample volume V, the chlorophyll content chl of the sample, and the fluorescence absorption parameter Q, the fluorescence flux F in (13) is expressed as

$$F = \gamma_f\,\sigma\,\Phi_f \quad \text{with} \quad \gamma_f := I_m\,chl\,V\,(1-Q) . \qquad (21)$$

The new parameter γ_f represents the gain of the PAM fluorometer and is expressed in units of [$g_{chl}\,V\,\mu E^{-1}$].

Model calibration is performed by formulating a dynamic parameter estimation problem, which is solved in the model development environment gPROMS (`http://www.psenterprise.com`) using maximum likelihood estimation.

4.1 Parameter Estimation Results

From the available data, three independent observations can be used to carry out parameter estimation, namely the fluorescence fluxes F', F'_0 and F'_m. In order to account for the accuracy of the PAM fluorometer, a 2% relative error is assumed for all the flux measurements.

Given the rather large number of parameters in the proposed model—15 parameters in total—not all of these parameter can be estimated with reasonable confidence from a single PAM experiment. Here, we decided to fix 5 of them: (i) the parameters k_r and τ in the Han model equal to the mean values of the ranges reported in (Han et al., 2000); (ii) the total number N of PSUs equal to the value found in (Falkowski and Raven, 1997); (iii) the characteristic time ξ of the qE quenching dynamics (8) according to (Maxwell and Johnson, 2000; Baker, 2008); and (iv) the fluorometer gain γ_f, whose value is clearly dependent on the PAM fluorometer used. The nominal values for these parameters are summarized in Table 1.

Table 1. Fixed parameter values.

Parameter	Value	Units
k_r	5.55×10^{-5}	s^{-1}
τ	5.55×10^{-3}	s
N	4.50×10^{-7}	$\mu E\, g_{chl}^{-1}$
γ_f	7.50×10^{-1}	$g_{chl}\, \mu E^{-1} V^{-1}$
ξ	5.00×10^{-2}	s^{-1}

The calibration results for the fluorescence fluxes are presented in Fig. 2. The corresponding parameter estimates are given in Table 2, together with their 95% confidence intervals.
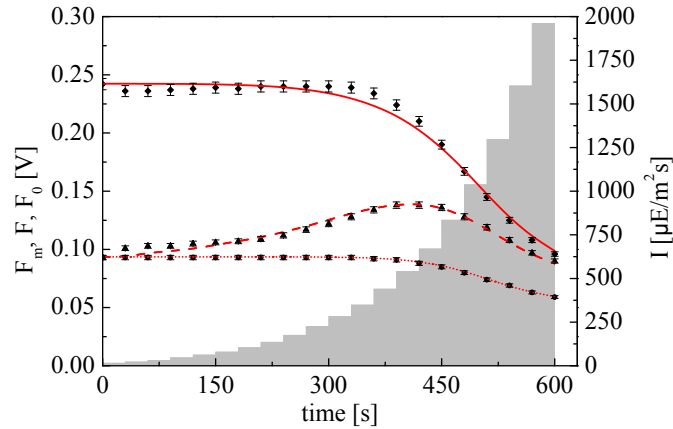

Fig. 2. Comparison between the predicted and measured fluorescence fluxes F'_m (diamonds, solid line), F'_0 (circles, dotted line) and F' (triangles, dashed line), in response to various actinic light levels I (grey-shaded area).

The fluorescence indexes q_L and q_{NPQ} can be computed based on (4) and (5) and using the calibrated parameter values in Table 2. These predictions are compared to the fluorescence indexes derived directly from the data in Fig. 3. The error bars on this plot are constructed by propagating the 2% relative error of the fluxes through (4) and (5).

Table 2. Parameter estimates and corresponding confidence intervals.

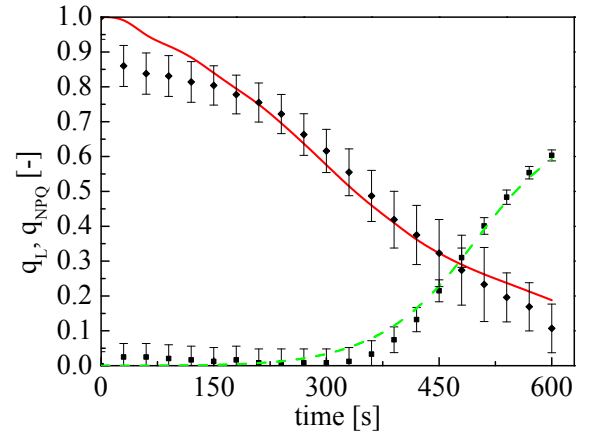| Parameter	Estimate	95% Conf. Int.	Units
Φ_f^A	2.89×10^{-2}	$\pm 2.16 \times 10^{-3}$	-
Φ_f^B	7.47×10^{-2}	$\pm 5.55 \times 10^{-3}$	-
k_d	4.51×10^{-6}	$\pm 5.94 \times 10^{-7}$	-
σ_{max}	4.33×10^{0}	$\pm 3.11 \times 10^{-1}$	$m^2\, g_{chl}^{-1}$
σ_{min}	2.53×10^{0}	$\pm 2.36 \times 10^{-1}$	$m^2\, g_{chl}^{-1}$
n	3.32×10^{0}	$\pm 6.08 \times 10^{-1}$	s^{-1}
I_{qE}	7.95×10^{2}	$\pm 5.95 \times 10^{1}$	$\mu E\, m^{-2}\, s^{-1}$

Fig. 3. Comparison between the predicted and measured fluorescence indexes q_L (diamonds, solid red line) and q_{NPQ} (squares, dashed green line).

Finally, using (18) in Property 1 and the calibrated parameter values for Φ_f^A and Φ_f^B in Table 2, an estimate of the quantum yield of an open RCII is obtained as $\Phi_p^A \approx 0.614$.

4.2 Discussions

The calibration results confirm the capability of the proposed model to accurately describe PAM fluorescence protocols, thereby providing a first validation of the model structure and underlying modelling assumptions. The estimated parameter values are in good agreement with those reported in the literature (Huot and Babin, 2010; Falkowski and Raven, 1997) and are obtained within acceptable confidence levels. We note that different parameters than those in Table 1 could be fixed and different values could be used for these parameters, which would modify the estimated parameter values in turn. Nonetheless, the resulting quality of fit would remain similar.

The Lake model appears to be providing accurate predictions of the fluorescence fluxes, suggesting a nonlinear relationship between the realized quantum yield of photosynthesis Φ_{PS2} and the fractions A, B of open and closed RCII's (Property 1). The predicted fluorescence indexes q_L and q_{NPQ} too are in good agreement with the experimental data, and the estimated quantum yield of an open RCII $\Phi_p^A \approx 0.615$ is close to other values reported in the literature (Sforza et al., 2012).

The photoregulation extension of the Han model, formulated in terms of the NPQ activity variable α taking values between 0 and 1, carries a mechanistic concept of activation/deactivation of NPQ. Accurate predictions of the available data could be obtained despite the as-

sumption of a constant characteristic time $\xi = 0.05$ s^{-1} in (8). We performed additional calibrations for ξ in the range $[0.005, 0.5]$ and noted that equally good fits could be obtained in all cases, yet with different estimates for certain parameters. For further discrimination, the results of a simulated experiment are shown in Fig. 4, whereby a constant actinic light is applied to a sample of dark-adapted microlagae. The transient behavior of the NPQ activity variable α is consistent with current literature data (Maxwell and Johnson, 2000; Baker, 2008) for ξ in a range between 0.01 and 0.1 s^{-1}; outside this range, the NPQ dynamics are found to be either too slow or too fast.
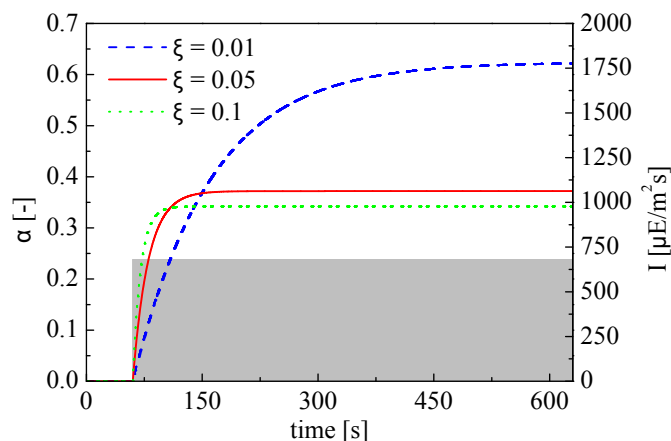

Fig. 4. Predicted NPQ activity α (color lines) for a constant actinic light (grey-shaded area).

5. CONCLUSIONS AND FUTURE WORK

This paper has presented a model of chlorophyll fluorescence that couples fast photochemical processes with photoregulation activity. This model builds upon the Han model that describes the fast dynamics of photoproduction and photoinhibition, and it encompasses NPQ regulation in the form of qE quenching. Moreover, an expression of the quantum yield of fluorescence has been proposed, based on which the characteristic fluorescence fluxes arising from PAM experiments can be related to the model variables and parameters. A first validation of this model has been undertaken, showing adequate agreement with characteristic fluorescence fluxes measured with a PAM fluorometer for the microalgae *Nannochloropsis Salina*. These results are certainly encouraging, yet they call for further validation with additional data, under steady-state and diverse dynamic conditions, in order to increase the total number of estimated parameters.

The proposed model is among the first of its kind to relate characteristic fluorescence parameters to PSU states. As such, it may also be helpful in unveiling and untangling various photosynthetic mechanisms. As well as fluorescence fluxes, the use of classical photosynthetic observations, such as oxygen production and biomass growth, is naturally possible, thereby widening the scope of validation against multiple experimental data sets from a variety of sources. Future directions involve accounting for more photoregulation processes (besides qE quenching) as well as extending the model to encompass photoacclimation and nutrient utilization (Hartmann et al., 2013).

REFERENCES

Baker, N.R. (2008). Chlorophyll fluorescence: A probe of photosynthesis in vivo. *Annual Review of Plant Biology*, 59(1), 89–113.

Benemann, J.R. (1997). CO_2 mitigation with microalgae systems. *Energy Conversion and Management*, 38, Supplement(0), S475 – S479.

Bilger, W. and Björkman, O. (1990). Role of the xanthophyll cycle in photoprotection elucidated by measurements of light-induced absorbance changes, fluorescence and photosynthesis in leaves of hedera canariensis. *Photosynthesis Research*, 25(3), 173–185.

Chisti, Y. (2007). Biodiesel from microalgae. *Biotechnology Advances*, 25(3), 294–306.

Falkowski, P.G. and Raven, J.A. (1997). *Aquatic photosynthesis*, volume 256. Blackwell Science Malden, MA.

Genty, B., Briantais, J.M., and Baker, N.R. (1989). The relationship between the quantum yield of photosynthetic electron transport and quenching of chlorophyll fluorescence. *Biochimica et Biophysica Acta (BBA) - General Subjects*, 990(1), 87 – 92.

Han, B.P. (2002). A mechanistic model of algal photoinhibition induced by photodamage to photosystem-II. *Journal of Theoretical Biology*, 214(4), 519–27.

Han, B.P., Virtanen, M., Koponen, J., and Straškraba, M. (2000). Effect of photoinhibition on algal photosynthesis: a dynamic model. *Journal of Plankton Research*, 22(5), 865–885.

Hartmann, P., Nikolaou, A., Chachuat, B., and Bernard, O. (2013). A dynamic model coupling photoacclimation and photoinhibition in microalgae. In *European Control Conference (ECC'13)*. July 17-19, 2013, Zürich, Switzerland.

Huot, Y. and Babin, M. (2010). Overview of fluorescence protocols: theory, basic concepts, and practice. In *Chlorophyll a Fluorescence in Aquatic Sciences: Methods and Applications*, 31–74. Springer.

Kramer, D., Johnson, G., Kiirats, O., and Edwards, G. (2004). New fluorescence parameters for the determination of q(a) redox state and excitation energy fluxes. *Photosynthesis Research*, 79(2), 1209–218.

le B. Williams, P.J. and Laurens, L.M.L. (2010). Microalgae as biodiesel & biomass feedstocks: Review & analysis of the biochemistry, energetics & economics. *Energy & Environmental Science*, 3(5), 554–590.

MacIntyre, H.L., Kana, T.M., Anning, T., and Geider, R.J. (2002). Photoacclimation of photosynthesis irradiance response curves and photosynthetic pigments in microalgae and cyanobacteria1. *Journal of Phycology*, 38(1), 17–38.

Maxwell, K. and Johnson, G.N. (2000). Chlorophyll fluorescence - a practical guide. *Journal of experimental botany*, 51(345), 659–668.

Metting, F.B. (1996). Biodiversity and application of microalgae. *Journal of Industrial Microbiology & Biotechnology*, 17, 477–489.

Müller, P., Li, X.P., and Niyogi, K.K. (2001). Non-photochemical quenching. a response to excess light energy. *Plant Physiology*, 125(4), 1558–1566.

Mutanda, T., Ramesh, D., Karthikeyan, S., Kumari, S., Anandraj, A., and Bux, F. (2011). Bioprospecting for hyper-lipid producing microalgal strains for sustainable biofuel production. *Bioresource Technology*, 102(1), 57–70.

Pittman, J.K., Dean, A.P., and Osundeko, O. (2011). The potential of sustainable algal biofuel production using wastewater resources. *Bioresource Technology*, 102(1), 17 – 25.

Sforza, E., Simionato, D., Giacometti, G.M., Bertucco, A., and Morosinotto, T. (2012). Adjusted light and dark cycles can optimize photosynthetic efficiency in algae growing in photobioreactors. *PloS one*, 7(6), e38975.

Sheehan, J., Dunahay, T., Benemann, J., and Roessler, P. (1998). A Look Back at the U.S. Department of Energy's Aquatic Species Program – Biodiesel from Algae. Technical report, U.S. Department of Energy.